
Research article

Numerical and experimental investigation for analyzing the temperature influence on the performance of photovoltaic module

Abdulrahman Th. Mohammad^{1,*} and Wisam A. M. Al-Shohani²

¹ Middle Technical University, Baqubah Technical Institute, Baghdad, Iraq

² Middle Technical University, Technical Engineering Collage, Baghdad, Iraq

* **Correspondence:** Email: abd20091976@gmail.com, abd20091976@mtu.edu.iq; Tel: +9647723482910.

Abstract: The effect of temperature is considered a significant factor in controlling the output voltage of the photovoltaic (PV) module. In this work, a numerical analysis with an experimental demonstration were investigated to analyze the temperature effect on the performance of PV module. In the numerical part, the current-voltage I-V and power-voltage P-V curves of the PV module were simulated under the influence of various module temperature ranged from 25 to 65 °C as well as various solar radiation from 200 to 1000 W/m². In addition, the variation of PV output electrical characteristics with a module temperature were performed to analyze the temperature coefficients of the PV module. Moreover, the experimental demonstration was performed to analyze performance of the PV module under the real weather conditions of Iraq. The numerical results conclude that the maximum power was recorded 165 W at 1000 W/m² solar irradiance and 25 °C PV module temperature. Furthermore, the temperature coefficient was recorded a maximum value with output power about (−0.26) %/°C. Besides, the experimental results show that the maximum power was recorded 131.2 W at solar irradiance about 920 W/m².

Keywords: photovoltaic module; modelling; temperature and irradiance influence; temperature coefficients; maximum power

Nomenclatures: *A*: PV module area (m²); *E_g*: Energy gap of the semiconductor (eV); FF: Fill factor (%); *I_D*, *I_O*, *I_{ph}*, *I_{mp}*, *I_{RS}*, *I_{sc}*, *I_{mo}*: Diode, saturation, photo-generated, maximum power point, reverse saturation, short circuit and module currents (A); *k*: Boltzmann constant 1.380649×10^{-23} (J K⁻¹); *n*:

Ideality factor; N_p , N_s : Number of cells in parallel and series; P : Electrical power (kW); q : Electronic charge = $1.602176634 \times 10^{-19}$ (Coulombs); R_s, R_{sh} : Series and Shunt resistance (Ohm); S : Solar irradiance (W/m^2); S_{ref} : Reference solar radiation ($1000 \text{ W}/\text{m}^2$); T_c : Cell temperature ($^{\circ}\text{C}$); T_{ref} : Reference temperature ($25 \text{ }^{\circ}\text{C}$); $V, V_T, V_{MO}, V_{mp}, V_{oc}$: Diode, thermal, module, maximum power point, open circuit voltages (V)

Greek Symbols: η : Electrical efficiency(%); $\alpha, \beta, \delta, \gamma$: Temperature coefficient of short circuit current, open circuit voltage, fill factor and maximum power ($\%/^{\circ}\text{C}$)

1. Introduction

The photovoltaic phenomenon is the most important technology that has been used to benefit from sun energy. It was used to convert solar energy into electrical directly through the so-called solar cell [1]. As a result of the development that took place in this field, the researchers have begun to develop and improve the performance of different types of solar cells like multi-junction, perovskite, and quantum [2–5]. Generally, the output electrical characteristics of PV solar cells are directly affected by the temperature variation. Whereas, the efficiency of the PV cell/module decreased with increasing the temperature [6,7] by 0.5% for each $1 \text{ }^{\circ}\text{C}$ [8,9]. Therefore, the influence of temperature variation on the behavior of PV cell/module should be described by the indicator of temperature coefficient. Where, the module temperature positively effects on the short circuit current (I_{sc}) and negatively on both open circuit voltage (V_{oc}), maximum power (P_{max}) and fill factor (FF) [10]. In indoor conditions, the method of measuring coefficient of temperature is considered inaccurate due to the difference between the characteristics of sun light spectrum and the light that used in simulator of test [11]. In the same manner, inaccuracy of outdoor test occurs because it is not possible to obtain a uniform change in the increasing of sunlight [12]. In open circuit, the temperature coefficient is assumed to be equal to 80–90% of temperature coefficient of maximum power [13] and can be calculated according to the assumption that the energy gap linearly change with the temperature range. While, in maximum power, the temperature coefficient is defined as the summation of temperature coefficient of the I_{sc} , V_{oc} , and FF [14]. The main characteristics of indoor and outdoor measurements can be summarized according to: (1) the PV cell in indoor test is illuminated with solar simulator, and (2) the temperature of the solar cell should be stable with $\pm 2 \text{ }^{\circ}\text{C}$ and temperature range should be at least $30 \text{ }^{\circ}\text{C}$ [15,16]. Besides, the oscillating of irradiance in outdoor should be kept within $\pm 2\%$ from the total solar irradiance, the wind speed not exceed 2 m/s , and the PV module temperature should be kept with $\pm 2 \text{ }^{\circ}\text{C}$ of ambient temperature. According to the literatures review, a number of researchers were presented numerical and experimental studies to analyse the influence of temperature on the PV module performance. The experimental studies were divided between indoor and outdoor measurements. For example, Indra [17] studied the influence of temperature on the output characteristics of the polycrystalline PV module. The outdoor tests show that the maximum power decreased by 17% with changing the PV module temperature from 15 to $60 \text{ }^{\circ}\text{C}$. Moreover, Amelia et al. [18] investigated the effect of operating temperature on the PV module mono-crystalline type. At first, the manufactured output characteristics of the PV was simulated by PV_{syst} software. Furthermore, outdoor experiments were investigated using I-V tracer (PROVA 200). In addition, the temperature distribution is determined using a digital thermal camera. The outdoor results showed that a variation of output characteristics of the PV module compared with STCs whereas the output power and the efficiency of the PV module decreases with the increasing of the

PV working temperature. Different types of the PV modules were tested indoor and outdoor by [16] to measure the temperature coefficients of I_{sc} and V_{oc} . The results of indoor test showed that a good agreement of the temperature coefficient with the results of the outdoor results. Singh and Ravindra [19] studied the influence of the temperature between 25 to 250 °C on the output characteristics of various types of PV modules. Their study was proved that the increasing of temperature lead to decrease each of the V_{oc} , FF and efficiency. According to Jehad Adeb et al. [20] study, the thin film module has less affected by increasing the temperature with less temperature coefficient about 0.0984% as compared with the other types. Where, the temperature coefficients were recorded 0.109%, for Mono-crystalline and -0.124% for Poly-crystalline. Based on the above literature review, it can be conclude that there is a relationship between the PV temperature and the outputs of the PV module, and can be determine the effects of the temperature on the PV output by indoor and outdoor tests. However, it can be seen that there is a limitation of using numerical analysis to determine the effects of the temperature on the PV outputs. For that, the main objective of this work is to study and analyze the effect of temperature on the output electrical characteristics of polycrystalline PV module using a numerical model validated by experimental test. In the numerical model, the I-V and P-V curves of the PV module were presented under the effect of module temperature ranges from 25 to 65 °C and solar irradiance ranges from 200 to 1000 W/m² using MATLAB software. In addition, the validation of the simulation results are performed with experimental results for the PV module under real weather conditions using I-V tracer (SEAWARD PV200).

2. Mathematical model

2.1. PV cell/module characteristics

The PV module is a group of solar cells connected in series or in parallel combination. Each cell has approximately 0.5 V. The electrical circuit of PV cell can be represented as shown in Figure 1.

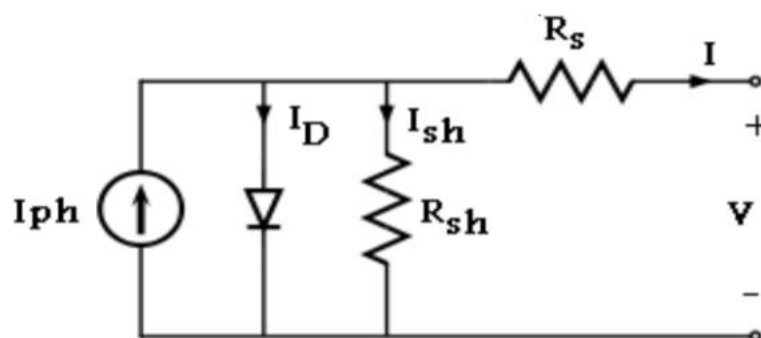


Figure 1. Electrical circuit of PV cell [21].

From Shockley equation [22,23], the current and voltage of PV cell in zero illumination can be represented by:

$$I_D = I_0 \left(e^{\left(\frac{V}{nV_T} \right)} - 1 \right) \quad (1)$$

where: V is the voltage across the cell, V_T is the thermal voltage (kT/q), q is the electronic charge = $1.602176634 \times 10^{-19}$ coulombs, T_c is the cell temperature ($^{\circ}\text{C}$), k is the Boltzmann constant = 1.380649×10^{-23} J K $^{-1}$ and n is the ideality factor of diode.

I_0 is the diode saturation current (A) and can be defined as [24]:

$$I_0 = I_{RS} \left(\frac{T_c}{T_{ref}} \right)^3 e^{\left(\frac{qE_g \left(\frac{1}{T_{ref}} - \frac{1}{T_c} \right)}{n k} \right)} \quad (2)$$

where I_{RS} is the reverse saturation current at STCs and E_g is the energy gap of the semiconductor used in the cell.

With the sunlight, the current of the solar cell is offset due to the photo current as [25,26]:

$$I = I_{ph} - I_0 \left(e^{\left(\frac{qV}{n k T} \right)} - 1 \right) \quad (3)$$

where: I_{ph} is the photo-generated current (A) and expressed as [27]:

$$I_{ph} = \frac{S}{S_{ref}} [I_{sc} + \alpha(T_c - T_{ref})] \quad (4)$$

where: S is the instantaneous solar irradiance (kW/m 2), S_{ref} is the reference solar irradiance (1 kW/m 2), I_{sc} is the short circuit current at STCs and α is the temperature coefficient of the I_{sc} .

In case of series resistance, the current generation described by [28]:

$$I = I_{ph} - I_0 \left(e^{\left(\frac{q(V-IR_S)}{n k T} \right)} - 1 \right) \quad (5)$$

where: R_S is the series resistance due to resistance of the silicon-bulk and contact material.

In case of parallel and series resistance, the current generation described by:

$$I = I_{ph} - I_0 \left(e^{\left(\frac{q(V+IR_S)}{n k T} \right)} - 1 \right) - \frac{V+IR_S}{R_{sh}} \quad (6)$$

where: R_{sh} is the shunt resistor due to inhomogeneity of the surface and loss-current at the solar cell edges.

The voltage of the solar cell can be written as:

$$V = -IR_S + k \log \left[\frac{I_{ph} - I + I_0}{I_0} \right] \quad (7)$$

Equation 7 can be written in term of PV module as [24]:

In case of PV cells in series:

$$V_{mo} = -I_{mo} N_S R_S + N_S k \log \left[\frac{I_{ph} - I_{mo} + I_0}{I_0} \right] \quad (8)$$

In case of PV cells in parallel:

$$V_{mo} = -I_{mo} \frac{R_S}{N_p} + k \log \left[\frac{N_S I_{ph} - I_{mo} + N_p I_0}{N_p I_0} \right] \quad (9)$$

where: *mo* represents the abbreviation of module, N_S and N_p are the number of cells in series and parallel respectively.

Generally, production power of the PV module can be defined as [29]:

$$P = N_S \times N_p \times V \times I \quad (10)$$

while, the efficiency can be defined as [30]:

$$\eta = \frac{P}{S \times A} \quad (11)$$

where: A is a PV module area.

The fill factor represents the ratio of maximum power to the theoretical [30]:

$$FF = \frac{I_{mp} V_{mp}}{I_{sc} V_{oc}} \quad (12)$$

where I_{mp} and V_{mp} are the current and voltage at maximum power point.

2.2. Temperature coefficients

The PV module efficiency depends on many types of losses. These losses can be confined as: thermalisation, transmission, emission, and angular mismatch and Carnot losses [10]. The increasing of PV temperature has a negative effect on these types of losses and can be represented by a temperature coefficients [31]. Commonly, the temperature coefficient is measured in indoor conditions and listed in the datasheet of the PV module. It can be classified into: I_{sc} , V_{oc} , FF and P_{max} coefficients.

The coefficient of temperature for I_{sc} [10], V_{oc} [32], FF [33,34] and for P_{max} [14] can be represented by equations from 13 to 16 respectively.

$$\alpha = \frac{I_{sc}(T_C) - I_{sc}(T_{ref})}{T_C - T_{ref}} \quad (13)$$

$$\beta = \frac{V_{oc}(T_C) - V_{oc}(T_{ref})}{T_C - T_{ref}} \quad (14)$$

$$\delta = \frac{1}{FF} \frac{dFF}{dT} \quad (15)$$

$$\gamma = \alpha + \beta + \delta \quad (16)$$

3. Experimental details

A polycrystalline PV module made by Fortuner (FRS-165W) was selected in this study to achieve the experimental tests. The PV module is fixed on a steel frame with tilt angle 33° towards the south depending on the latitude of site as shown in Figure 2. The main specifications of the PV module is presented in Table 1. I-V tracer (SEAWARD PV200) was used to measure the output electrical characteristics of the PV module including I_{sc} , V_{OC} , V_{mp} , I_{mp} , and P_{max} . Furthermore, a solar meter (Survey 200R) device was synchronized with the SEAWARD PV200 to measure the ambient conditions (air temperature and solar radiation) and back temperature of module. All the measured data were stored in a computer and reviewed by solar data logger and then displayed by SolarCert software. The wind speed was measured by a handle anemometer. In addition, an infrared thermal digital camera (visual IR thermometer VT02) was used to image of temperature distribution on the front and back sides of the PV module.

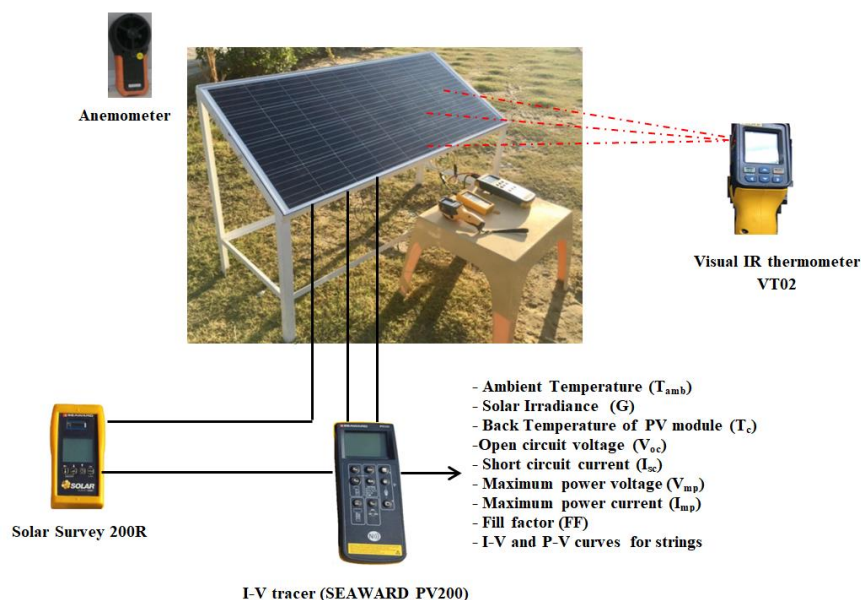


Figure 2. Diagram of the outdoor test.

Table 1. Technical data of the PV module.

Parameter	Value
Dimensions	149×67 cm
P_{max}	165 W
I_{sc}	9.81 A
V_{oc}	22.05 V
I_{mp}	9.17 A
V_{mp}	18 V
η	

4. Weather data

Iraq is considered one of the hot and dry countries in the summer season. Where, the maximum temperature reaches almost more than 50 °C, especially in August month. Four days (1/8/2021, 5/8/2021, 11/8/2021 and 13/8/2021) were selected to measure the parameters of the PV module. As shown in Figure 3, the maximum average ambient temperature was reached about 51 °C at noon between (1:00 pm and 2:00 pm). Besides, the average solar radiation was recorded a maximum value about 940 W/m² at noon as shown in Figure 4. While, the average wind velocity was not exceed 0.5 m/s in the morning at 6:00 am as shown in Figure 5.

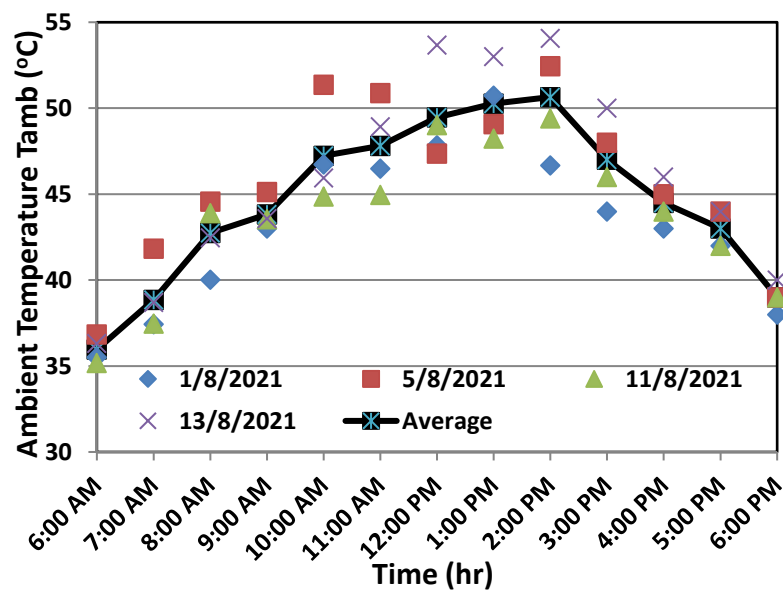


Figure 3. Variation of ambient temperature during the test.

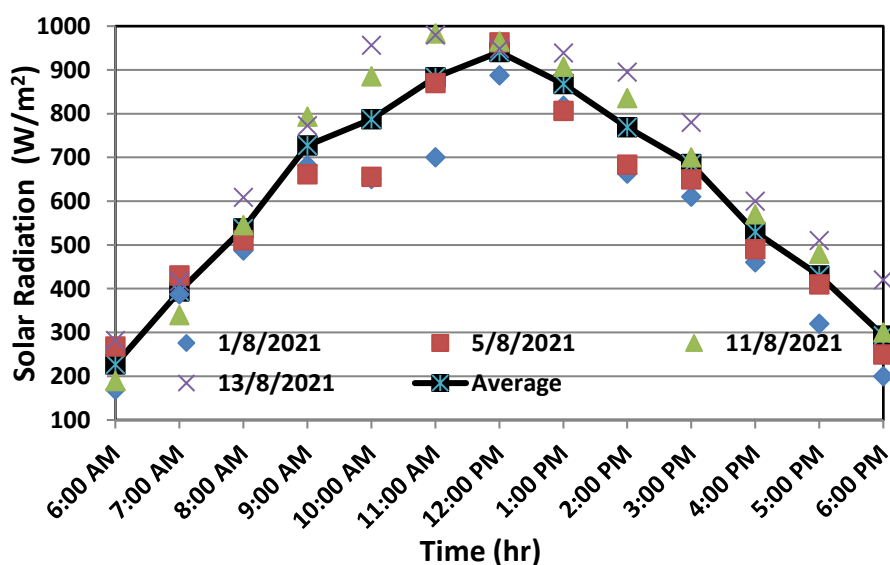


Figure 4. Variation of solar radiation during the test.

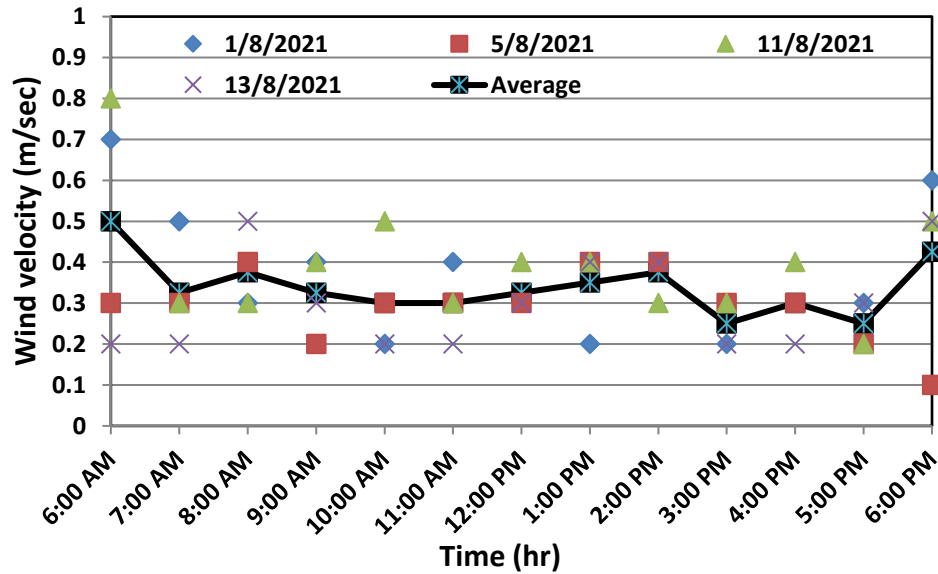


Figure 5. Variation of wind speed during the test.

5. Results and discussion

5.1. Numerical results

A MATLAB code was built based on the set of Eqs (1–16) and the technical data of PV module that tabulated in Table 1 to analyse the I-V and P-V curves of the PV module. In addition, the variation of V_{OC} , I_{sc} , P_{max} and FF were represented with module temperature to analyze the temperature coefficients. The I-V and P-V curves were represented in ranges of module temperature and solar radiation between (25 to 65) °C and (200 to 1000) W/m². While, the analysis of temperature coefficients were investigated at (600, 800, and 1,000) W/m². As shown in Figure 6, the I_{sc} was varied from (9.6 to 9.8) A when the module temperature was changed from (25 to 65) °C at constant solar radiation 1000 W/m². While, the V_{oc} was decreased from (22.05 to 20.2) V resulting in a maximum power changed from (146 to 165) W as shown in Figure 7. It is observed that the increasing the temperature of PV module has critical effect on decreasing the voltage rather than increasing the current. This can be explained as follows: Increasing cell temperature lead to reduce of band gap energy, which indicates to increase the absorbed photons that results in producing more free charge carriers. In other words, lower energy needs to liberate the free charge carrier. This means that the number of flow electrons with more current and low energy will increase (drop in voltage) [30,35].

On the other side, at constant temperature (25 °C) and solar radiation varied from (200 to 1000) W/m², the I_{sc} , V_{OC} were varied from (2 to 9.8) A and from (20.1 to 22.05) V respectively resulting in a maximum power range from (31 to 165) W as shown in Figures 8 and 9.

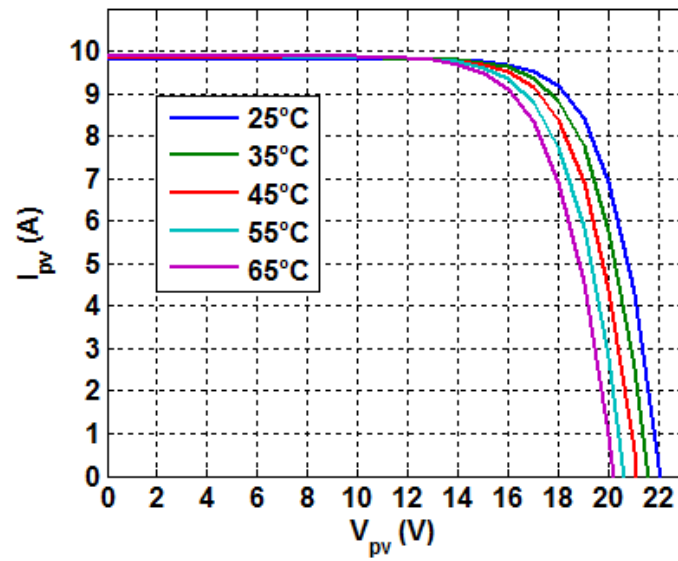


Figure 6. I-V curve of PV module at 1000 W/m^2 .

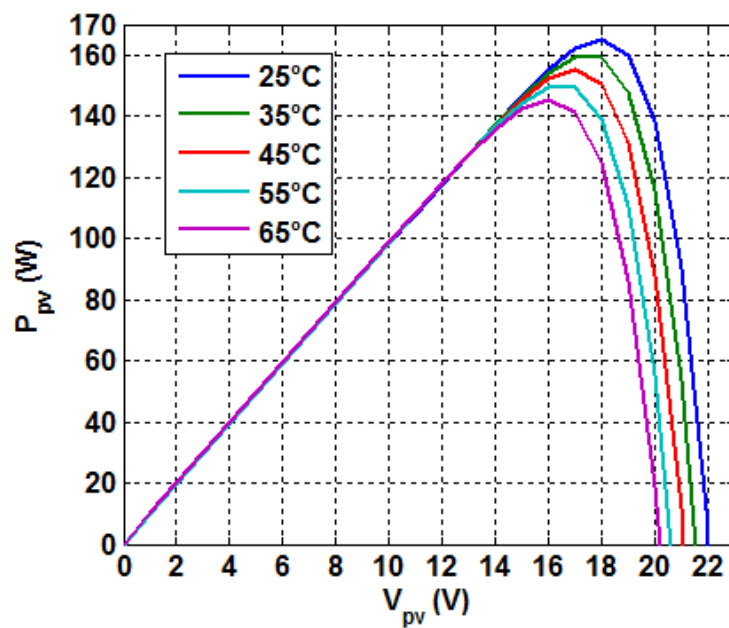


Figure 7. P-V curve of PV module at 1000 W/m^2 .

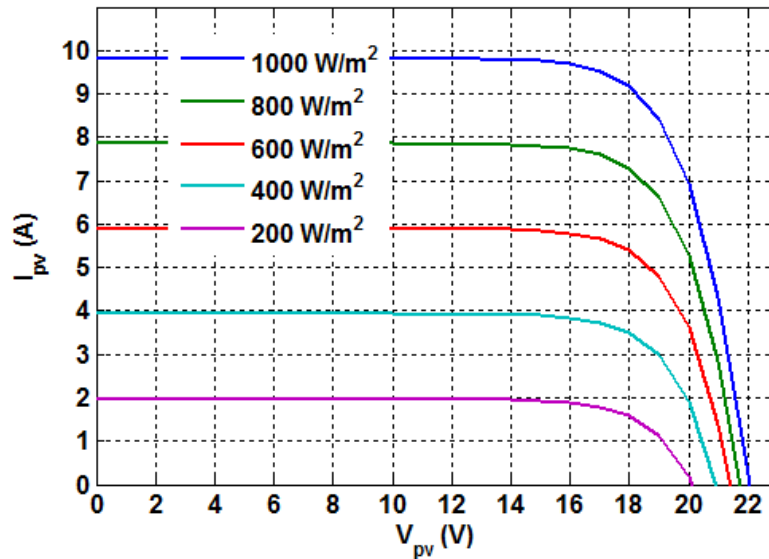


Figure 8. I-V curve of PV module at 25 °C.

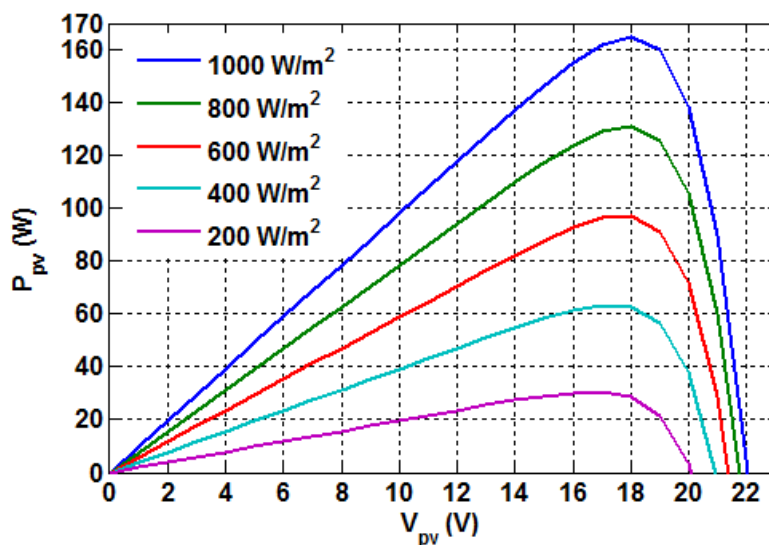


Figure 9. P-V curve of PV module at 25 °C.

The variation of output characteristics such as: I_{sc} , V_{oc} , P_{max} , and FF with the module temperature are plotted in Figures (10–13) for three values of solar radiation (600, 800 and 1,000) W/m^2 . As shown in figures, the relationship seems to be a linear model with increasing trend in I_{sc} and decreasing trend in V_{oc} , P_{max} , and FF . The temperature coefficients were calculated from the slop of straight lines presented in Table 2. As shown, the temperature coefficient (α) of I_{sc} was obviously changed from 0.058 to 0.091 $\%/^{\circ}C$ when the solar radiation increased from 600 to 1000 W/m^2 . While, the temperature coefficient (β) of V_{oc} , (γ) of P_{max} and (δ) of FF were little changed. As presented in Table 2, the regression equations of module are characterized by a high coefficient of determination (R^2) with a range from 0.962 to 0.999. This is an indication that this regression correlation can be used to predict the output electrical characteristics of the PV module.

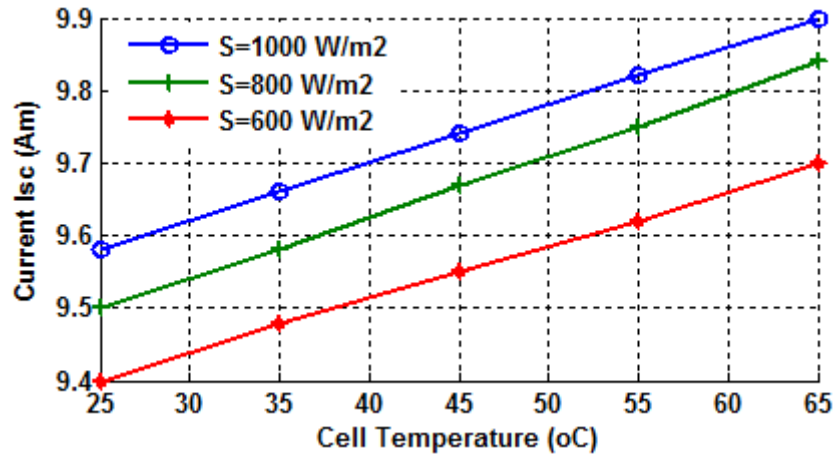


Figure 10. Variation of I_{sc} with PV module temperature.

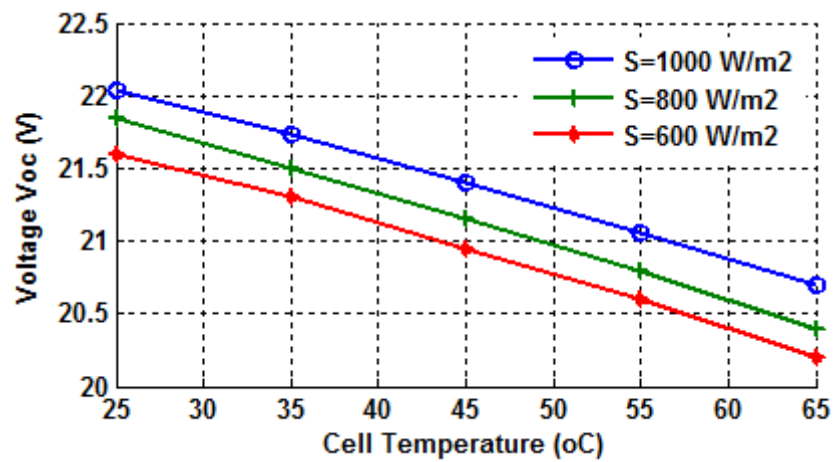


Figure 11. Variation of V_{oc} with PV module temperature.

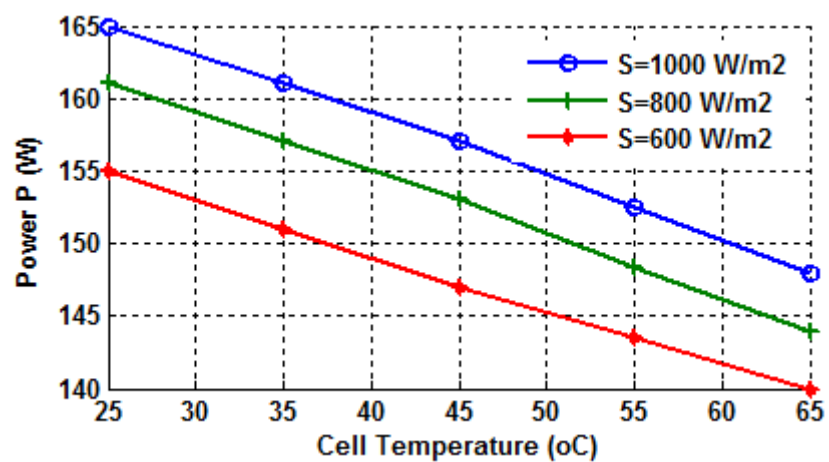


Figure 12. Variation of P_{max} with PV module temperature.

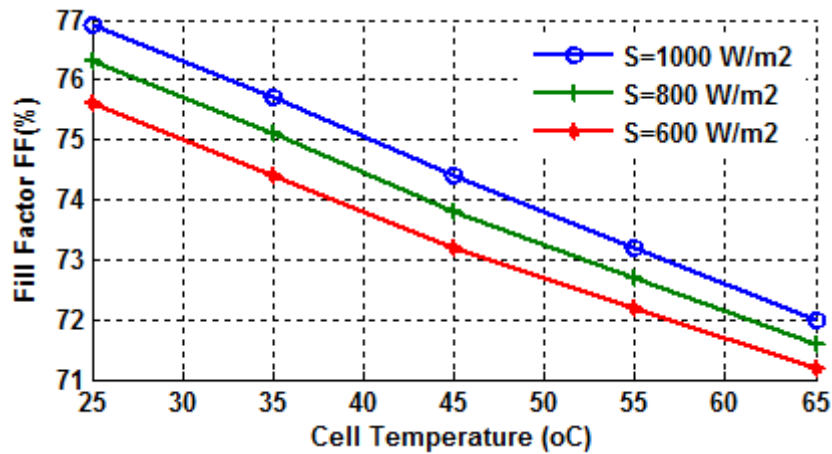


Figure 13. Variation of FF with PV module temperature.

Table 2. Linear models of output characteristics and temperature coefficient.

Solar radiation W/m ²	Linear models and temperature coefficients			
	I_{sc} (A)	V_{oc} (V)	FF (%)	P (W)
1000	$I_{sc} = 0.008 * T_c + 9.38$	$V_{oc} = -0.034 * T_c + 23$	$FF = -0.120 * T_c + 80$	$P = -0.43 * T_c + 180$
	$\alpha = 0.0815\%/^{\circ}C$	$\beta = -0.15\%/^{\circ}C$	$\delta = -0.155\%/^{\circ}C$	$\gamma = -0.26\%/^{\circ}C$
	$R^2 = 0.9992$	$R^2 = 0.994$	$R^2 = 0.989$	$R^2 = 0.993$
800	$I_{sc} = 0.0085 * T_c + 9.285$	$V_{oc} = -0.036 * T_c + 23$	$FF = -0.12 * T_c + 79$	$P = -0.43 * T_c + 170$
	$\alpha = 0.086\%/^{\circ}C$	$\beta = -0.163\%/^{\circ}C$	$\delta = -0.155\%/^{\circ}C$	$\gamma = -0.26\%/^{\circ}C$
	$R^2 = 0.9996$	$R^2 = 0.987$	$R^2 = 0.979$	$R^2 = 0.997$
600	$I_{sc} = 0.0074 * T_c + 9.217$	$I_{sc} = -0.035 * T_c + 23$	$FF = -0.11 * T_c + 78$	$P = -0.38 * T_c + 160$
	$\alpha = 0.075\%/^{\circ}C$	$\beta = -0.158\%/^{\circ}C$	$\delta = -0.142\%/^{\circ}C$	$\gamma = -0.23\%/^{\circ}C$
	$R^2 = 0.9993$	$R^2 = 0.986$	$R^2 = 0.989$	$R^2 = 0.988$

5.2. Experimental results

5.2.1. Temperature of PV module

The experimental investigation was investigated during four days of August (01/08/2021), (05/08/2021), (11/08/2021) and (13/08/2021) from 6:00 am to 2:00 pm at the center of Middle Technical University-Baghdad, Iraq. The output characteristics of PV module such as: I_{sc} , I_{mp} , V_{oc} , V_{mp} , P_{max} , FF , and electrical efficiency (η_{ele}) in addition to its back temperature were measured as shown in Figure 14. From figure, the maximum value of PV temperature was recorded about 69 °C in 13/08/2021 at 1:00 pm while the minimum temperature was recorded about 37 °C in 01/08/2021 at 6:00 am. According to the average value, the PV module temperature was recorded about 37.5 °C and 63 °C as a minimum and maximum value respectively. The module temperature was varied due to the variation of solar radiation and ambient temperature.

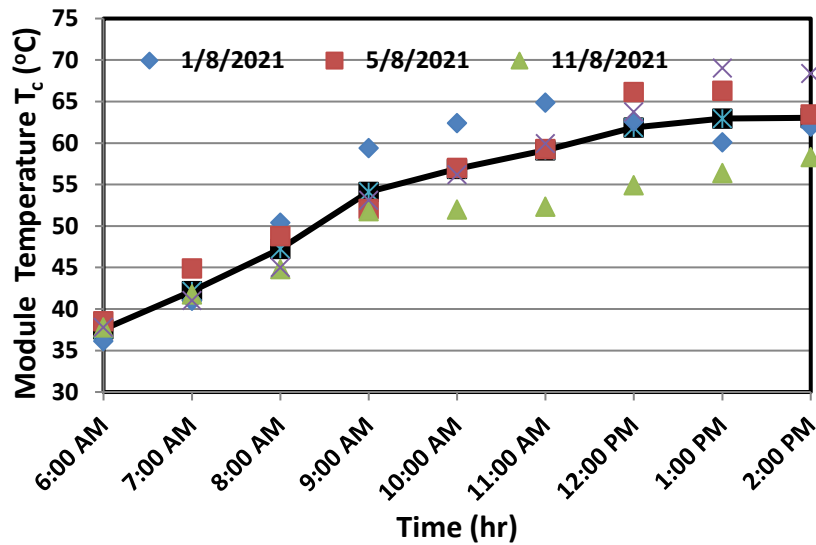
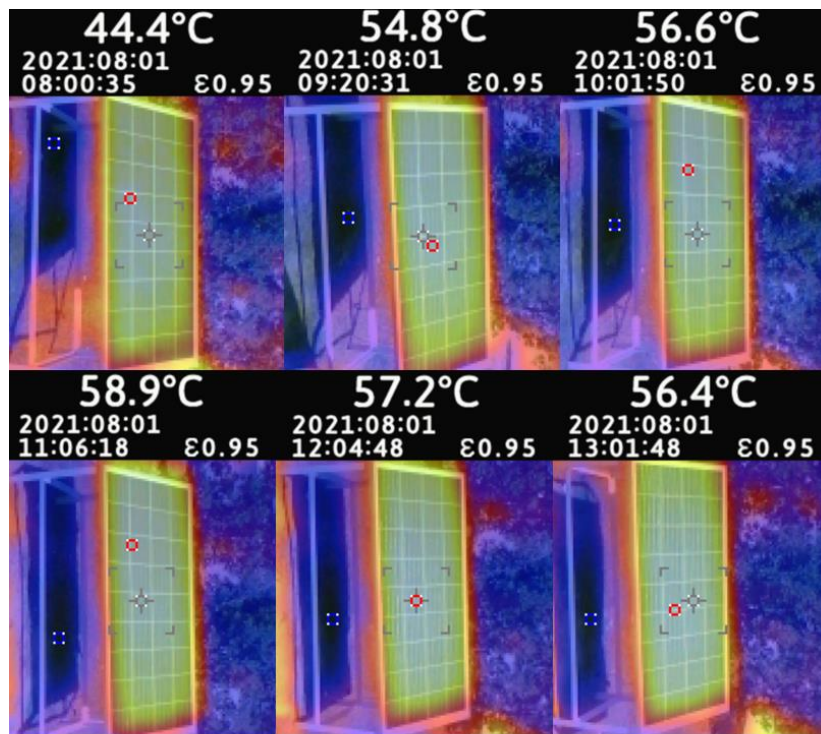
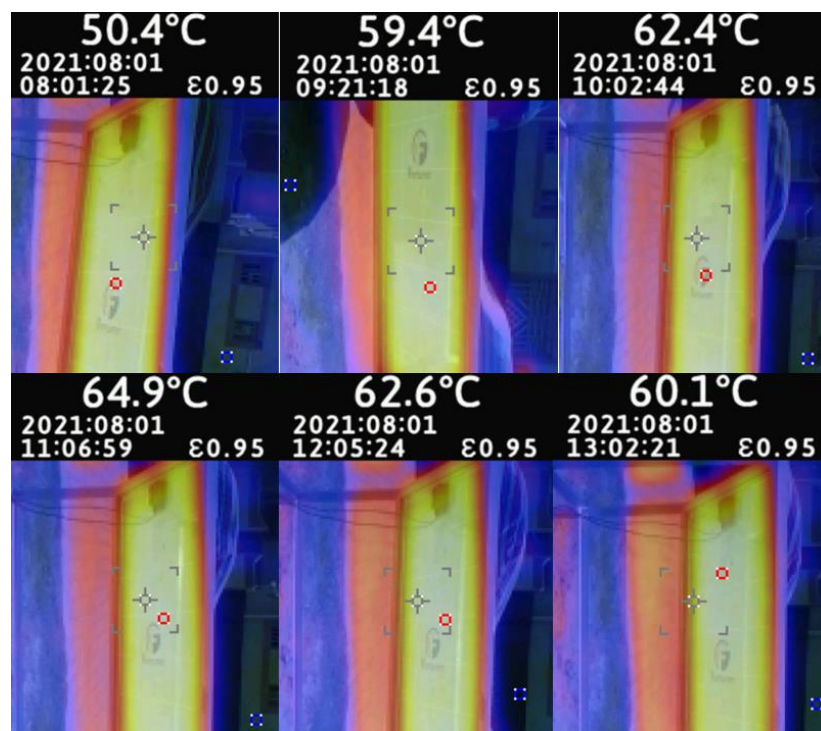


Figure 14. Variation of module temperature during the test.

Furthermore, the front and back temperatures of the PV module were imaged using thermal digital camera for one day 01/08/2021 to compare between them as shown in Figure 15. The images were taken every one hour between 8:00 am to 1:00 pm. Generally, the PV back temperature was recorded a higher than the front temperature. Where, the maximum temperature of front and back was recorded 58.9 °C and 64.9 °C respectively at 11:00 am. This can be explained by the fact that the PV module was installed at average height not exceeding 1m from the ground surface (i.e., it closer to the ground) therefore, the air currents were very low. In addition, more heat will reflect from the ground surface toward the back surface of module.



a) Thermal images of front PV module



b) Thermal images of back PV module

Figure 15. Thermal image of front and back temperatures of PV module.

5.2.2. Output electrical characteristics

Figure 16 shows the variation of module voltage with time. As shown, the V_{oc} was slightly decrease from 20.75 to 20.35 V while, the V_{mp} was sharply decrease from maximum value 18.55 to 15.9 V due to the higher increase of module temperature. In contrast to this, the I_{sc} and I_{mp} were increased. Where, the I_{sc} was increased from 1.72 to 7.32 A while, I_{mp} was increased from 1.4 to 6.9 A as shown in Figure 17.

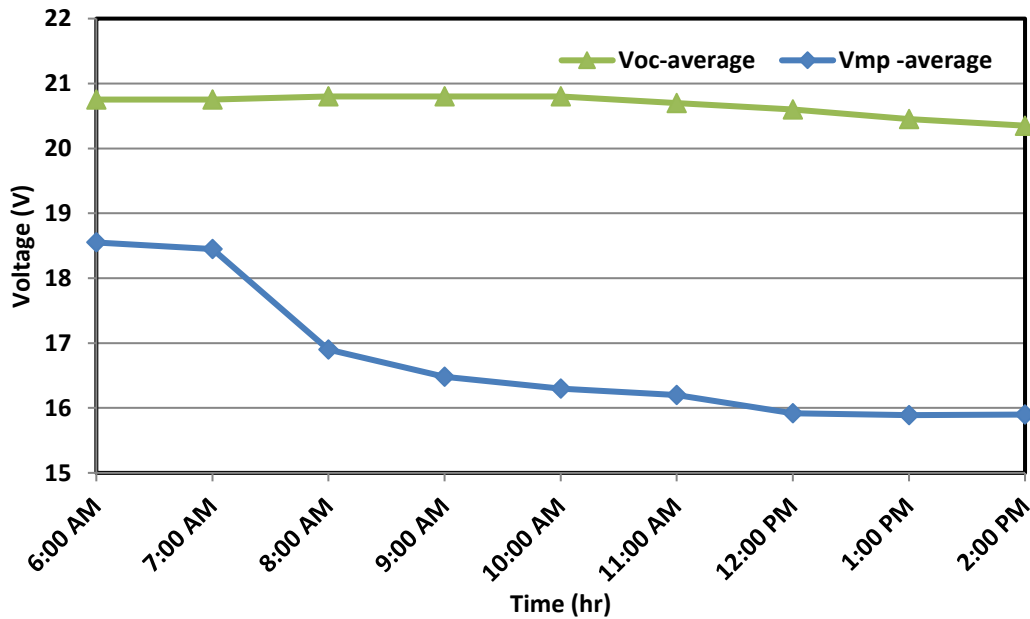


Figure 16. Variation of voltage during the test.

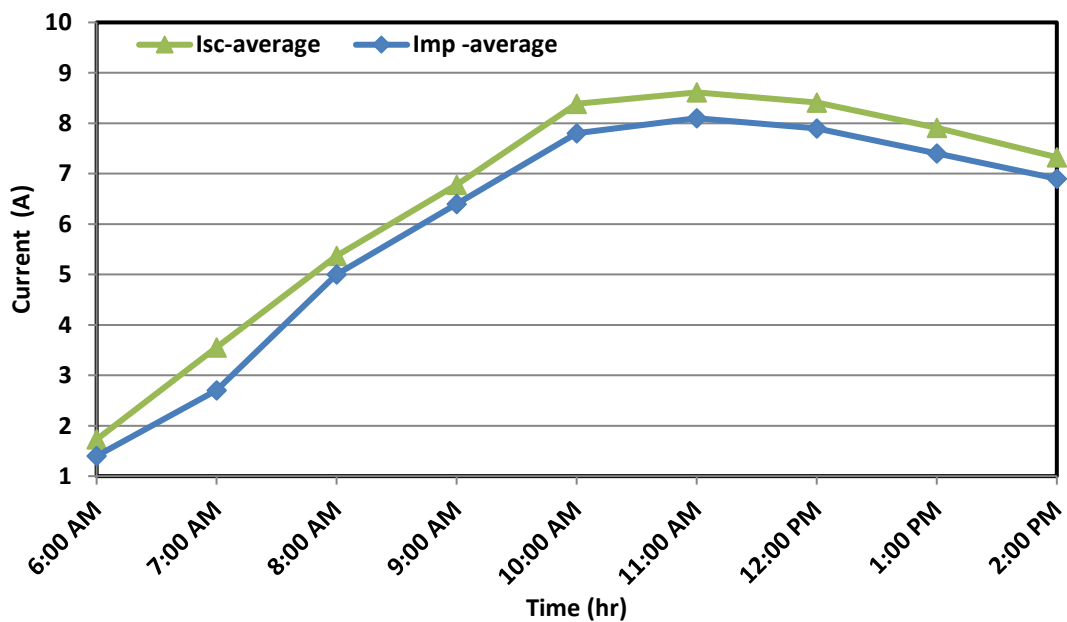


Figure 17. Variation of current during the test.

As shown in Figure 4, the average solar irradiance was increased from 220 to 920 W/m² during 6:00 am to 12:00 pm. Therefore, the electrical power was increased from 25.9 to 131.2 W then dropped to 109.7 W at 2:00 pm because of decreasing the solar irradiance to 770 W/m² as shown in Figure 18. This is accompanied by a decline in the electrical efficiency (η_{ele}) of the module from 15.6% to 13.3% and decreasing in fill factor from 76% to 71%.

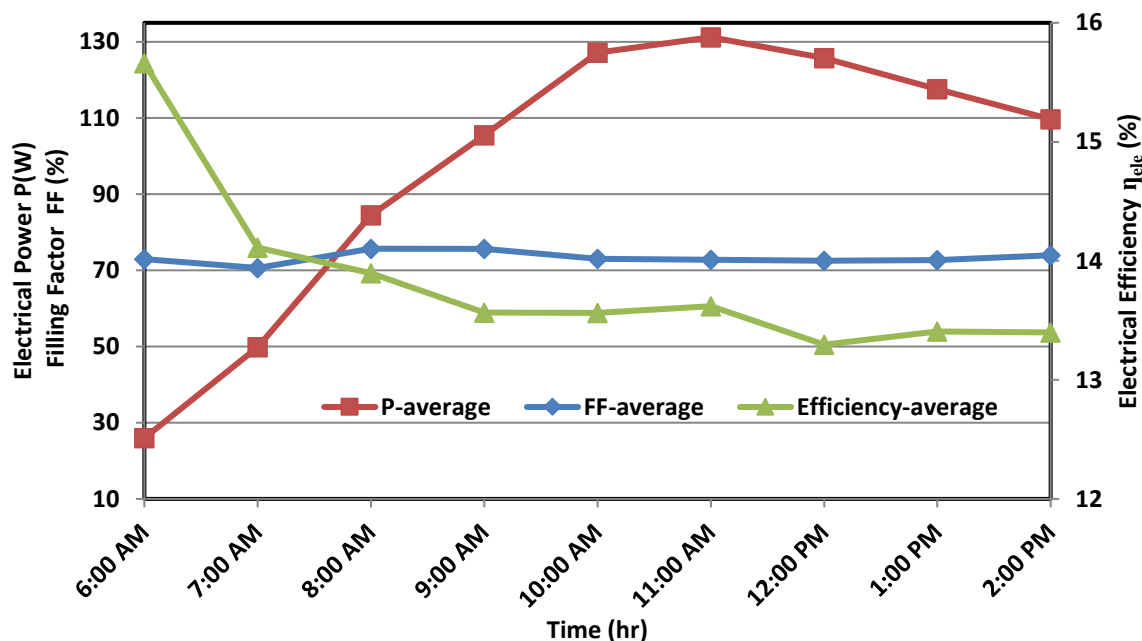


Figure 18. Variation of power, filling factor, and efficiency during the test.

5.3. Comparative of present results with previous studies in literature

The temperature coefficients of current, voltage and maximum power were compared with same studies in literature [10,15,36] as presented in Table 3. The comparison was depended on the same type of PV modules (polycrystalline) that found in the previous studies. The structure of table was built according to technical data of PV module, ambient conditions and temperature coefficients. As presented in Table 3, the temperature coefficient of current (α) was close to the coefficient temperature in [36] at solar radiation 1000 W/m² while, the coefficients of voltage (β) and power max (γ) were recorded greater than those in [36]. In the same manner, all the temperature coefficients in present study recorded less than the coefficients of reference [10]. Otherwise, they recorded greater than the coefficients in reference [15]. On the other side, the linear model with Coefficient of Determination (R^2) of the current, voltage and power equations were compared also with [36] at 1000 W/m² as shown in Table 4. The comparison shows a good agreement between the two studies since the R^2 value was very close.

Table 3. Comparison of temperature coefficients with previous studies.

Ref.	Technical data	Country	Type of study	Solar radiation W/m ²	Temp. Module °C	Temperature coefficients %/°C			
						α (I_{sc})	β (V_{oc})	δ (FF)	γ (P_{max})
[36]	$V_{oc} = 44.9$ V $I_{sc} = 5.75$ A $V_{mp} = 36.2$ V $I_{mp} = 5.11$ A $P_{max} = 80$ W	Thailand	Exp. Outdoor	1000	40–65	0.08181	-0.05185	NA	-0.00038
[10]	$V_{oc} = 0 - 50$ V $I_{sc} = 0 - 15$ A $P_{max} > 10$ W	Norway	Exp. Outdoor	> 400	10–70	0.171	-0.23	-0.42	-0.47
[15]	NA	Nepal	Numerical	1000	15–60	0.001	-0.073	-0.20	-0.132
Present study	$V_{oc} = 22.05$ V			1000		0.0815	-0.150	-0.155	-0.260
	$I_{sc} = 9.81$ A			800		0.0860	-0.163	-0.155	-0.260
	$V_{mp} = 18$ V $I_{mp} = 9.17$ A	Iraq	Numerical	600	25–65	0.0750	-0.158	-0.142	-0.230
	$P_{max} = 165$ W								

Table 4. Comparison of linear model accuracy of present study with previous studies at 1000 W/m².

Reference	I_{sc} (A)	V_{oc} (V)	P_{max} (W)
[36]	$I_{sc} = 0.0121 * T_c + 7.0092$ $R^2 = 0.9945$	$V_{oc} = -1.2393 * T_c + 304.03$ $R^2 = 0.9982$	$P = -0.0077 * T_c + 2.44423$ $R^2 = 0.9934$
Present study	$I_{sc} = 0.008 * T_c + 9.38$ $R^2 = 0.9992$	$V_{oc} = -0.034 * T_c + 23$ $R^2 = 0.9940$	$P = -0.43 * T_c + 180$ $R^2 = 0.9930$

5. Conclusions

The output electrical characteristics of PV module were investigated by numerical and experimental studies. In addition the temperature coefficients of PV module was analyzed numerically. Based on the analyses of the results, the following conclusions can be drawn:

- The numerical results conclude that the maximum power was recorded 165 W at 1000 W/m² solar irradiance and 25 °C PV module temperature.
- The increasing of module temperature has critical effect on the voltage rather than the current.
- The minimum value of power was recorded about 31 W at 200 W/m² of solar radiation.
- The temperature coefficient was recorded a maximum value with output power about (-0.26) %/°C. While, the temperature coefficient (β) of V_{oc} , (γ) of P_{max} and (δ) of FF were little changed.
- The experimental results show that the maximum power was recorded 131.2 W at 920 W/m² solar radiation.

Acknowledgments

This work was conducted within Middle Technical University and the authors are grateful to the staff of University for their help.

Conflict of interest

The authors demonstrate that there is no conflict of interest regarding this manuscript.

References

1. Sim M, Suh D (2021) A heuristic solution and multi-objective optimization model for life-cycle cost analysis of solar PV/GSHP system: A case study of campus residential building in Korea. *Sustainable Energy Technol Assess* 47: 101490. <https://doi.org/10.1016/j.seta.2021.101490>
2. Zhang C, Gwamuri J, Andrews R, et al. (2014) Design of multijunction photovoltaic cells optimized for varied atmospheric conditions. *Int J Photoenergy* 2014: 1–7. <https://doi.org/10.1155/2014/514962>
3. Ahmad K, Khan MQ, Kim H (2022) Simulation and fabrication of all-inorganic antimony halide perovskite-like material based Pb-free perovskite solar cells. *Opt Mater* 128: 112374. <https://doi.org/10.1016/j.optmat.2022.112374>
4. Ahmad K, Khan MQ, Khan RA, et al. (2022) Numerical simulation and fabrication of Pb-free perovskite solar cells (FTO/TiO₂/Cs₃Bi₂I₉/spiro-MeOTAD/Au). *Opt Mater* 128: 112458. <https://doi.org/10.1016/j.optmat.2022.112458>
5. Aissat A, Arbouz H, Nacer S, et al. (2016) Efficiency optimization of the structure pin-InGaN/GaN and quantum well-InGaN for solar cells. *Int J Hydrogen Energy* 41: 20867–20873. <https://doi.org/10.1016/j.ijhydene.2016.06.028>
6. Fterich M, Chouikhi H, Sandoval-Torres S, et al. (2021) Numerical simulation and experimental characterization of the heat transfer in a PV/T air collector prototype. *Case Stud Therm Eng* 27: 101209. <https://doi.org/10.1016/j.csite.2021.101209>
7. Ali OM (2020) An experimental investigation of energy production with a hybrid photovoltaic/thermal collector system in Duhok city. *Case Stud Therm Eng* 21: 100652. <https://doi.org/10.1016/j.csite.2020.100652>
8. Penmetsa V, Holbert KE (2019) Climate change effects on solar, wind and hydro power generation. *In 2019 North American Power Symposium (NAPS):* 1–6. <https://doi.org/10.1109/NAPS46351.2019.9000213>
9. Almashary B, Telba A (2018) Effect of high temperature to output power of solar cell. *Proceedings of the World Congress on Engineering, Vol I WCE 2018*, July 4–6, 2018, London, U.K. Available from: http://www.iaeng.org/publication/WCE2018/WCE2018_pp304-308.pdf.
10. Paudyal BR, Imenes AG (2021) Investigation of temperature coefficients of PV modules through field measured data. *Sol Energy* 224: 425–439. <https://doi.org/10.1016/j.solener.2021.06.013>
11. Photovoltaic Devices-Part 3 (2016) Measurement principles for terrestrial photovoltaic (PV) solar devices with reference spectral irradiance data, IEC 60904-3. Available from: <https://webstore.iec.ch/publication/61084>.

12. Landis GA (1994) Review of solar cell temperature coefficients for space. In: *XIII Space Photovoltaic Research and Technology Conference (SPRAT XIII)*, 1994, 385. Available from: <https://ntrs.nasa.gov/citations/19950014125>.
13. Green MA (2003) General temperature dependence of solar cell performance and implications for device modelling. *Photovoltaics Res Appl* 11: 333–340. <https://doi.org/10.1002/pip.496>
14. Dupr'e O, Vaillon R, Green M (2015) Physics of the temperature coefficients of solar cells. *Sol Energy Mater Sol Cells* 140: 92–100. <https://doi.org/10.1016/j.solmat.2015.03.025>
15. Tayyib M, Ove J, Oskar T (2014) Irradiance dependent temperature coefficients for MC solar cells from Elkem solar grade silicon in comparison with reference polysilicon. *Energy Procedia* 55: 602–607. <https://doi.org/10.1016/j.egypro.2014.08.032>
16. Dubey R, Batra P, Chattopadhyay S (2015) Measurement of temperature coefficient of photovoltaic modules in field and comparison with laboratory measurements. In: *2015 IEEE 42nd Photovoltaic Specialist Conference (PVSC)*, 1–5. <https://doi.org/10.1109/PVSC.2015.7355852>
17. Indra Bahadur Karki (2015) Effect of temperature on the I-V characteristics of a polycrystalline solar cell. *J Nepal Phys Soc* 3: 35–40. <https://doi.org/10.3126/jnphysoc.v3i1.14440>
18. Amelia AR, Irwan YM, Leow WZ, et al. (2016) Investigation of the effect temperature on photovoltaic (PV) panel output performance. *Int J Adv Sci Eng Inf Technol* 6: 682–688. <https://doi.org/10.18517/ijaseit.6.5.938>
19. Singh P, Ravindra NM (2012) Temperature dependence of solar cell performance-an analysis. *Sol Energy Mater Sol Cells* 101: 36–45. <https://doi.org/10.1016/j.solmat.2012.02.019>
20. Adeeb J, Farhan A, Al-Salaymeh A (2019) Temperature effect on performance of different solar cell technologies. *J Ecol Eng* 20: 249–254. <https://doi.org/10.12911/22998993/105543>
21. Salmi T, Bouzguenda M, Gastli A, et al. (2012) MATLAB/Simulink based modelling of solar photovoltaic cell. *Int J Renewable Energy Res* 2: 213–218. Available from: <http://www.ijrer.org/ijrer/index.php/ijrer/article/view/157>.
22. Walker GR (2001) Evaluating MPPT converter topologies using a MATLAB PV model. *J Electr Electron Eng* 21: 49–56. Available from: <https://espace.library.uq.edu.au/view/uq:59100>.
23. Naeijian M, Rahimnejad A, Ebrahimi SM, et al. (2021) Parameter estimation of PV solar cells and modules using Whippy Harris Hawks Optimization Algorithm. *Energy Rep* 7: 4047–4063. <https://doi.org/10.1016/j.egy.2021.06.085>
24. Shukla A, Khare M, Shukla KN (2015) Modeling and simulation of solar PV module on MATLAB/Simulink. *Int J Innovative Res Sci, Eng Technol* 4: 18516–1852. <https://doi.org/10.1088/1757-899X/114/1/012137>
25. Villalva MG, Gazoli JR, Filho ER (2009) Comprehensive approach to modeling and simulation of photovoltaic arrays. *IEEE Trans Power Electron* 24: 1198–1208. Available from: <https://ieeexplore.ieee.org/document/4806084>.
26. Hishikawa Y, Doi T, Higa M (2018) Voltage-Dependent temperature coefficient of the I-V curves of crystalline silicon photovoltaic module. *IEEE J Photovoltaic* 8: 48–53. <https://doi.org/10.1109/JPHOTOV.2017.2766529>
27. Ayaz R, Nakir I, Tanrioven M (2014) An improved matlab-simulink model of pv module considering ambient conditions. *Int J Photoenergy*, 1–6. <https://doi.org/10.1155/2014/315893>

28. Khanh LN, Seo JJ, Kim YS, et al. (2010) Power-management strategies for a grid-connected PV-FC hybrid system. *Power Delivery, IEEE Trans* 25: 1874–1882. <https://doi.org/10.1109/TPWRD.2010.2047735>
29. Erdem Z, Erdem MB (2013) A Proposed model of photovoltaic module in Matlab/Simulink™ for distance education. *Procedia-Social Behav Sci* 103: 55–62. <https://doi.org/10.1016/j.sbspro.2013.10.307>
30. Cotfas DT, Cotfas PA, Machidon OM (2018) Study of temperature coefficients for parameters of photovoltaic cells. *Int J Photoenergy*, 1–12. <https://doi.org/10.1155/2018/5945602>
31. Duck B, Fell C, Anderson K, et al. (2018) Determining the value of cooling in photovoltaics for enhanced energy yield. *Sol Energy* 159: 337–345. <https://doi.org/10.1016/j.solener.2017.11.004>
32. Bellini A, Bifaretti S, Iacovone V, et al. (2009) Simplified model of a photovoltaic module. In *Proceedings of the Applied Electronics (AE '09), Pilsen, Czech Republic, September*: 47–51. Available from: <https://ieeexplore.ieee.org/document/5289294>
33. Berthod C, Strandberg R, Yordanov GH, et al. (2016) On the variability of the temperature coefficients of mc-Si solar cells with irradiance. *Energy Procedia* 92: 2–9. <https://doi.org/10.1016/j.egypro.2016.07.002>
34. Qu H, Li X (2019) Temperature dependency of the fill factor in PV modules between 6 and 40 °C. *J Mech Sci Technol* 33: 1981–1986. Available from: <https://link.springer.com/article/10.1007/s12206-019-0348-4>.
35. Jha AR (2009) Solar cell technology and applications. CRC press: New York. <https://doi.org/10.1201/9781420081787>
36. Kamkird P, Ketjoy N, Rakwichian W, et al. (2012) Investigation on temperature coefficients of three types photovoltaic module technologies under thailand operating condition. *Procedia Eng* 32: 376–383. <https://doi.org/10.1016/j.proeng.2012.01.1282>



AIMS Press

© 2022 the Author(s), licensee AIMS Press. This is an open access article distributed under the terms of the Creative Commons Attribution License (<http://creativecommons.org/licenses/by/4.0>)